

1 **Interaction between silica particles with poly(ethylene oxide)**  
2 **studied using an optical tweezer: insignificant effect of**  
3 **poly(ethylene oxide) on long-range double layer interaction**

4

5 Lester C. Geonzon, Motoyoshi Kobayashi \*, Takuya Sugimoto, Yasuhisa Adachi

6 *Faculty of Life and Environmental Sciences, University of Tsukuba*

7 *1-1-1 Tennodai, Tsukuba, Ibaraki, 305-8572, Japan*

8

9

10

11

12 \*Corresponding author:

13 Name: Motoyoshi Kobayashi, Ph.D.

14 E-mail Address: [kobayashi.moto.fp@u.tsukuba.ac.jp](mailto:kobayashi.moto.fp@u.tsukuba.ac.jp)

15 Tel & Fax: +81-(0)29-853-5721

16 Address: Faculty of Life and Environmental Sciences, University of Tsukuba

17 1-1-1 Tennodai, Tsukuba, Ibaraki, 305-8572, Japan

18

19 **Abstract**

20 It is known that the adsorption of nonionic polymers or surfactants reduces the  
21 magnitude of zeta potential of colloidal particles and provides the steric repulsion  
22 between particles. A question remains as to whether nonionic polymers affect the  
23 structure of the electric double layer (EDL). To elucidate the effect of nonionic polymer  
24 on EDL, we investigated the long-range interaction forces between silica particles in  
25 aqueous solutions with different molecular weights of polyethylene oxide (PEO) having  
26 higher affinity to silica by using optical tweezers. For all measurements, long-ranged  
27 repulsive interactions were observed. The onset of the interaction force for bare  
28 particles and those with low molecular weight PEO remained identical and was  
29 consistent with the Derjaguin-Landau-Verwey-Overbeek (DLVO) predictions. This  
30 result indicates that the adsorption of nonionic PEO does not affect the charging  
31 properties of silica, and the interaction originates from the overlapping of the EDL.  
32 With high molecular weight PEO, the onset of interactions shifted to a few hundred  
33 nanometers larger than those for bare particles and was quantified using the Alexander-  
34 de Gennes model, suggesting the steric interactions originate from the protruding tails  
35 and/or loops of the adsorbed PEO layer. Based on the force measurements, we  
36 emphasize that the adsorption of nonionic polymer onto the surface of the silica  
37 particles does not affect the EDL surrounding the particles. Hence, we corroborate the  
38 notion that the reduction of the magnitude of zeta potential in the presence of nonionic  
39 polymer is attributable to the shift of the shear plane from the hydrodynamic viewpoint.

40 **Keywords:** DLVO/Steric interactions/Optical tweezers/PEO adsorption

## 41 **1. Introduction**

42 The control of the stability and rheology of dispersions of colloidal particles is  
43 essential in many applications, as in industrial products like paint, inks, food products  
44 like mayonnaise, chocolate, as well as cosmetics, and pharmaceutical formulations [1–  
45 4]. On the other hand, applications for flocculation of particles like water and  
46 wastewater treatments are also paramount[5, 6].

47 The stability and rheology of colloids are regulated by the interparticle forces[7, 8].  
48 Meanwhile, colloidal particles are charged and form an electric double layer (EDL).  
49 The sum of attractive van der Waals force and repulsive force due to the overlap of  
50 EDL is known as Derjaguin-Landau-Verwey-Overbeek (DLVO) force[9–13]. DLVO  
51 force is considered ubiquitous for charge stabilized colloids[6, 9, 14].

52 In most applications, the adsorbing polymers are usually added to the colloidal  
53 dispersions to control the stability and rheology[7, 8]. Polymers at interfaces are  
54 significantly important in many industrial applications[8, 15]. In general, polymer  
55 adsorption onto the colloidal particles can lead to various effects on the stability and  
56 rheology of their suspensions, ranging from steric stabilization to bridging flocculation,  
57 shear-thickening, and shear thinning, depending on several factors, including polymer  
58 concentration, electrolyte concentration, and polymer conformation at the surface [16,  
59 17]. Hence, the adsorbed polymers can be crucial in controlling the fate of the colloidal  
60 particles for different applications.

61 Electrokinetic techniques are widely used to characterize the surface charging  
62 properties of colloidal particles and surfaces [18–26]. From the electrokinetic  
63 measurements, so-called zeta potential, which is the electric potential at the plane of  
64 shear adjacent to the particles, can be extracted. Zeta potential with DLVO theory has  
65 been successfully used to explain the stability of the dispersion of bare colloidal  
66 particles [9, 13, 27–29]. The electrokinetic measurements are considered a standard  
67 technology, and the electrokinetics of bare particles are well studied. The presence of a  
68 polymer layer on the surface may affect the electrokinetic transport properties of the  
69 colloidal particle [22]. The adsorption of neutral polymers/surfactants on colloidal  
70 particles is reported to reduce the magnitude of zeta potential [7, 30–32]. For example,  
71 Garvey et al. [33] reported the rapid drop in the zeta-potential of latex particles with the  
72 addition of nonionic poly(vinyl alcohol) (PVA). This decrease is considered to originate  
73 from the adsorption of PVA onto the latex particles. Zaman [7] also reported the  
74 reduction of the zeta potential of silica particles with the addition of poly(ethylene  
75 oxide) (PEO). Meanwhile, Heiningen and Hill [34] reported the temporal decrease in  
76 the mobility magnitude of trapped silica microsphere with the adsorption of PEO using  
77 optical tweezers electrophoresis. In these studies, the reduction in the zeta potential or  
78 mobility magnitude is often interpreted by the outward shift of the location of the shear  
79 plane, and the shift is in some cases regarded as the thickness of adsorbed polymer  
80 layers [4, 22, 30, 31, 33–36]. Then, the thickness of the polymer layer is quantified from  
81 the reduction of zeta potential by assuming that the potential distribution in the EDL  
82 near the surface is hardly disturbed by the adsorbed polymer layer. The assumption

83 seems reasonable but has never been examined.

84 The objective of this research is to clarify if nonionic polymer affects EDL  
85 structure. Our idea in this paper is to measure DLVO interaction force at long-range  
86 distances in the presence and absence of nonionic polymers. Using optical tweezers  
87 allows us to measure the long-range and weak interaction forces between particles for  
88 bare and with an adsorbed polymer layer at the different molecular weights.  
89 Furthermore, we utilize silica particles and polyethylene(oxide) (PEO), having a higher  
90 affinity to silica surfaces, as a model particle and nonionic polymer. The interaction  
91 between silica surfaces in the presence of PEO has been studied using different force  
92 measurement techniques [7, 20, 32–39]. While many studies reported the effect of  
93 adsorbed PEO on the interaction forces between silica surfaces, the discussion is mostly  
94 focused on the steric interactions in the presence of PEO at the surface [39–43]. In the  
95 present study, the effect of diffuse double layer and steric interactions are differentiated  
96 by varying the molecular weight of PEO and background electrolyte concentration.  
97 Suppose the force curve with nonionic polymer PEO is similar to that without PEO. In  
98 that case, we can postulate that nonionic polymer PEO does not significantly affect  
99 EDL structure. Thus, the well-known reduction in zeta potential is due to the shift of  
100 the shear plane coming from a hydrodynamic problem with adsorbed polymers.  
101 Therefore, this study has aimed to provide a basis for the assumption and improve our  
102 understanding of the EDL structure in the presence of nonionic polymer.

103

## 104 **2. Materials and Methods**

## 105 **2.1 Materials**

106 The probe particles used in the experiments were non-functionalized silica  
107 particles (diameters  $2a=$  10.0 and 5.6  $\mu\text{m}$ , JGC Catalysts and Chemicals, Ltd.,  
108 Japan) suspended in deionized (DI) water (Elix Advantage 5, Millipore, Tokyo,  
109 Japan). Both particle suspensions were prepared by diluting the stock suspension  
110 of 0.01 wt.% to 0.0005 wt.%. Poly (ethylene oxide) (PEO) with a molecular  
111 weight of 1000 kg/mol and 100 kg/mol were purchased from Sigma Aldrich  
112 (Sigma Aldrich: St. Louis, MO). Poly(ethylene glycol) (PEG) with an average  
113 molecular weight of 20 kg/mol was purchased from Wako Pure Chemicals Ind.,  
114 Ltd. Stock polymer solutions ( $\sim$ 500 ppm) were prepared by dissolving the  
115 powders in DI with vigorous stirring at room temperature for two days and  
116 carefully covered to avoid photodegradation. The radii of gyration,  $R_g$ , of the  
117 polymers were estimated from the molecular weight following the reference [44,  
118 45], as shown in Table 1. All polymer stock solutions were used within two  
119 weeks, and stored at 5 °C. A 10 mM KCl solution was added to control the ionic  
120 strength of the samples.

## 121 **2.2 Optical tweezers set up**

122 An optical trapping kit (OTKB/M, Thorlabs) equipped with a single laser  
123 (wavelength  $\lambda=$ 976 nm) was used in the experiments, as described elsewhere[46, 47].  
124 A 100 $\times$  oil immersion objective with a high numerical aperture (NA 1.25, WD 0.23  
125 mm, Nikon) was used to tightly focus the laser beam and visualize the colloidal particle.

126 An air condenser then collected the trapping laser passing through the sample (10×, NA  
127 0.25, W.D. 7 mm, Nikon) and further reflected into the quadrant position detector  
128 (QPD) using a dichroic mirror for the back-focal plane detection (OTKBFM, Thorlabs).  
129 A piezo-controlled 3-dimension translational stage (NanoMax 300, Thorlabs) was used  
130 to position the microscope glass slide using the Thorlabs APT software package. We  
131 used a force measurement module (OTKBFM-CAL, Thorlabs) to record the QPD  
132 signals. The constant particle displacement was measured by image processing, and the  
133 QPD calibration factor was determined to be around 0.16 V/μm[46]. The stage  
134 displacement and the  $x$ - and  $y$ - displacement of the particle in the optical trap were  
135 recorded using a custom-made data acquisition program in LabVIEW software  
136 (National Instruments, Austin, TX).

### 137 **2.3 Force measurement**

138 The force measurement between two particles with different radii, as shown in Fig.  
139 1, was performed in a microscope cell separated by a double adhesive tape and sealed  
140 with a vacuum sealant following the reference with slight modifications [48, 49]. The  
141 vacuum sealant protects the sample from evaporation during the measurements. A  
142 particle  $A_1$  with radius  $a_1$  was optically trapped at a height equal to the radius of a large  
143 particle  $A_2$ ,  $a_2$ . The larger particle,  $A_2$ , was initially allowed to adhere to the cover glass  
144 by drying in a closed environment. Then, the cover glass was used to make the  
145 microscope cell. After that, the particle suspension of 0.0005 wt%, 5.6 μm particle was  
146 injected into the cell without or with 100 ppm of the polymer [42, 50, 51]. The sample

147 pH was measured to be around 6. The addition of an excess amount of polymer  
148 molecule is also expected to be adsorbed onto the large particles pre-adhered on the  
149 cover glass. The sample cell was kept for 10 minutes to develop adsorption on the  
150 adhered particles and obtain saturation. A free 5.6  $\mu\text{m}$  particle was then held in an  
151 optical trap for the measurements. We determined the initial surface-to-surface distance  
152 between particles by image processing and converted it from pixels to micrometers  
153 using microscope calibration scales.

154 Force measurement was performed by translating the adhered large particle via the  
155 piezo-controlled stage at a speed of 0.02  $\mu\text{m/s}$  using custom software in LabVIEW  
156 (National Instruments, Austin, TX). We assume no hydrodynamic interaction takes  
157 place at this slow translation speed. As the larger particle approaches the trapped  
158 particle, the trapped particle is displaced laterally from its equilibrium position,  $\Delta x$ ,  
159 which is detected by the QPD. The force is obtained from the lateral displacement  
160 measurement,  $k \Delta x$ , where  $k$  is the trap stiffness. The trap stiffness  $k$  was fixed at  
161  $2.35 \times 10^{-5}$  N/m in all force measurements. Force measurements were repeated for at  
162 least five different pairs of particles. All measurements were performed at room  
163 temperature, 20  $^{\circ}\text{C}$ .

### 164 **3. Results and Discussions**

#### 165 **3.1 Interaction forces between silica particles in KCl solutions**

166 The double-layer forces between bare silica particles in electrolyte concentrations  
167 were measured to validate the methodology. Figure 2 shows the experimental results of



168 direct force measurements between silica particles in dilute KCl concentration. When  
 169 the adhered particle approached the trapped particle at a constant speed of 0.02  $\mu\text{m/s}$ , a  
 170 repulsive force was observed for both KCl concentrations due to the overlapping of the  
 171 EDL, and the onset of repulsion decreased with the increasing electrolyte concentration.

172 To further evaluate the experimental force curve, the total interaction force  
 173 between the two colloidal particles was analyzed using the DLVO theory, wherein the  
 174 interparticle forces were governed by the electrostatic double-layer (EDL) force and the  
 175 van der Waals (VDW) attraction force:

$$176 \quad F_T = F_{\text{EDL}}(h) + F_{\text{VDW}}(h) \quad (1)$$

177 The EDL interactions for a sphere-sphere geometry with different sizes can be  
 178 described as follows:

$$179 \quad F_{\text{EDL}}(h) = \frac{128\pi N_A c_s k_B T \gamma^2}{\kappa} \left( \frac{a_1 a_2}{a_1 + a_2} \right) e^{-\kappa h} \quad (2)$$

180 where  $\frac{a_1 a_2}{a_1 + a_2}$  is the effective radius following Derjaguin's approximation with  $a_1$  and  
 181  $a_2$  are the particle radii,  $h$  is the surface-to-surface distance,  $N_A$  is Avogadro's number,  
 182  $c_s$  is the electrolyte concentration in mM,  $k_B T$  is the Boltzmann constant multiplied by  
 183 absolute temperature,  $T$ ,  $\gamma$  is given by  $\gamma = \tanh(ze\psi/4k_B T)$  where  $e$  is the elementary  
 184 charge,  $z$  is the valence of ions,  $\psi$  is the surface potential, and  $1/\kappa$  is the Debye length.

185 Meanwhile, the attractive VDW interaction is given as

$$186 \quad F_{\text{VDW}}(h) = \frac{-A_H}{6h^2} \left( \frac{a_1 a_2}{a_1 + a_2} \right) \quad (3)$$

187 where the  $A_H$  is the Hamaker constant between silica particles in an aqueous solution.  
 188 The  $A_H$  was set to  $2.0 \times 10^{-21}$  J; this value is within the reported values of the Hamaker  
 189 constant of silica in water [13, 52]. The theoretical DLVO force curve was compared to

190 the experimental data with  $\psi$  as a fitting parameter, and the  $\kappa$  was calculated directly  
191 from the electrolyte concentration of the solution.

192 In Fig. 2, the experimental and theoretical curves showed good agreement. From  
193 the fit of DLVO theory to the measured curves, the absolute surface potential was  
194 obtained to be around  $65.7 \pm 1.2$  mV and  $50 \pm 1.7$  mV for 0.1 mM and 0.5 mM KCl  
195 solutions, respectively. As the salt concentration increases, the onset of the double layer  
196 forces decreases at a surface-to-surface distance of around 250 nm and 150 nm for 0.1  
197 mM and 0.5 mM KCl due to the thinning of the diffuse double layer. The measured  
198 force curve and surface potential between silica particles using optical tweezers were  
199 consistent with the theoretical predictions and agreed with previous studies [13, 27].  
200 Hence, this agreement indicates that our methodology is sound for measuring long-  
201 range interactions between two particles.

### 202 **3.2 Interaction forces between silica particles with adsorbed PEO layer**

203 The addition of a PEO in the particle suspension would result in polymer  
204 adsorption onto the surface of the silica particle [8, 37, 42, 47, 53–56]. The interaction  
205 forces between two surfaces with the adsorbed polymer layers with different molecular  
206 weights were measured to evaluate the effect of PEO on the surface properties of the  
207 silica particles. Figure 3 presents the experimental results of direct force measurement  
208 between silica particles mediated with PEO of different molecular weights at 0.1 mM  
209 and 0.5 mM KCl. The force curve is purely repulsive for all particles mediated with  
210 PEO. At a low KCl concentration (0.1 mM), the force curve for a low molecular weight

211 PEO (20 kg/mol) converges quite well with the bare particles. Since the layer thickness  
212 of the adsorbed polymer, which is assumed to be around  $2R_g$ - $3R_g$  where  $R_g$  of a 20  
213 kg/mol PEO is estimated to be 7.6 nm (see Table 1), is thinner than the diffuse part of  
214 the double-layer structure, we postulate that the observed repulsion is dominated by the  
215 overlapping of diffuse double-layer. This resembles the interaction of silica particles  
216 even in the presence of the small molecule polymer adsorbed at the surface, and thus  
217 the force is governed by the overlapping of diffuse double-layer and is electrostatic in  
218 nature. Furthermore, increasing the molecular weight to 100 kg/mol with  $R_g$  estimated  
219 to be 17.1 nm (see Table 1), the force curve still converges with those for bare and with  
220 20 kg/mol adsorbed PEO layer. Therefore, similar to the interaction mediated with the  
221 20 kg/mol adsorbed PEO layer, we consider that the interaction originated from the  
222 EDL repulsion, and the adsorption of the nonionic polymer did not affect the surface  
223 property of the particles.

224 On the other hand, for a high molecular weight PEO, the onset of the interaction  
225 was shifted to a few hundreds of nanometers around to  $3R_g$ , significantly larger than  
226 those for bare particles and with a low molecular weight polymer. With the presence of  
227 a high molecular weight PEO, the thickness of the adsorbed polymer layer was  
228 expectedly thicker; hence when the two polymer-covered surfaces approach each other,  
229 the trapped particle experiences a force from the outer segments of the adsorbed  
230 polymer layer. Thus, the shift was attributed to the steric repulsion, and the onset of  
231 repulsion can be used to estimate the layer thickness of the adsorbed polymer layer [42].

232 The effect of double-layer structure and steric repulsion on the interaction between  
233 silica particles was further differentiated by increasing the background salt  
234 concentration. Increasing the salt concentration suppresses the EDL repulsion due to  
235 the charge screening. Figure 3b presents the force curve for bare and adsorbed polymer  
236 layers at 0.5 mM KCl concentration. The onset of the interaction force for bare silica  
237 particles and those mediated with 20 kg/mol PEO remained identical and shifted to a  
238 lower surface-to-surface distance. This observation is in line with those found for 0.1  
239 mM KCl background concentration. Since the layer thickness of the adsorbed polymer  
240 is still thinner than the diffuse double layer; thus, the interaction is driven by the  
241 overlapping of the EDL, and the adsorption of small molecular weight nonionic  
242 polymer does not alter the surface property of the particle. Moreover, a fluctuation in  
243 the force curve could be seen at large separation distance and may be a possibility of  
244 secondary minimum or depletion force in the presence of polymer. However, this is not  
245 the case in our measurements because the polymer size is small and the concentration  
246 of polymers is low. Hence, this could be an artifact since these forces are too weak and  
247 may be masked by the limitation of the force detection at very low forces. On the one  
248 hand, the onset of interaction for silica particles mediated with 1000 kg/mol PEO did  
249 not show significant differences from those in 0.1 mM KCl concentration. This implies  
250 that the steric interaction is also not affected by the change in the diffuse double-layer  
251 [35, 57, 58]. Hence, based on the above discussion, we consider that the adsorption and  
252 attachment of the PEO molecule on the surface of the silica particle do not affect the  
253 charge group at the surface and imply that the presence of nonionic polymer does not

254 influence the double-layer structure of the particles.

255 A similar observation was also reported by Giesbers et al. [41] using AFM between  
256 the polymer-covered sphere and polymer-covered plate, wherein the approach curve  
257 with low molecular weight PEO at  $10^{-3}$  M NaCl is dominated by electrostatic repulsion.  
258 Correspondingly, Wei et al. [39] observed a similar tendency in the interaction between  
259 latex particles and silica glass surface-mediated with PEO at low polymer concentration.  
260 Although reported, the consideration of the surface potential and the commonly  
261 observed reduction in the zeta-potential was not addressed. Moreover, the effect of PEO  
262 on the surface of silica particles has been studied using electrokinetic measurements[7,  
263 8,33, 36, 37]. It was shown that the absolute magnitude of zeta-potential ( $\zeta$ -potential)  
264 decreases with the increasing adsorbed amount of PEO. As mentioned in the  
265 introduction, electrokinetic measurements provide information on the surface  
266 properties of the charged particles; however, it is equally reliant on the hydrodynamic  
267 properties of the outermost region of the interface. Thus, the observed decrease in the  
268  $\zeta$ -potential somehow reflects the hydrodynamic properties of the adsorbed PEO layers.  
269 Since the long-range force measurements did not exhibit any significant changes in the  
270 surface properties of the particles in the presence of the nonionic polymer layer, we  
271 attribute that the adsorption of the nonionic polymer has almost no effect on the surface  
272 potential and EDL structure of charged silica particles, albeit the commonly reported  
273 change in the  $\zeta$  -potential. Therefore, based on the above discussion, we postulate that  
274 the reported decrease in the absolute magnitude of  $\zeta$ -potential in the presence of PEO  
275 was attributed to the shift of the shear plane from the hydrodynamic point of view as

276 schematically drawn in Fig. 4.

### 277 **3.3 Steric interactions by large molecular weight polymer**

278 The effect of steric repulsion by large molecular weight polymers was quantified  
279 using the Alexander-de Gennes (AdG) model [60, 61]. Following Derjaguin's  
280 approximation, the interaction force between two surfaces for the symmetric case of the  
281 AdG model is given as follows:

$$282 \quad F_{\text{symm}}(h) = \frac{8\pi k_B T L}{35s^3} \left( \frac{a_1 a_2}{a_1 + a_2} \right) \left[ 7 \left( \frac{2L}{h} \right)^{5/4} + 5 \left( \frac{h}{2L} \right)^{7/4} - 12 \right] \quad (4)$$

283 where  $k_B T$ ,  $a_1$ ,  $a_2$  and  $h$  are defined earlier, and  $L$  is originally defined as the thickness  
284 of the grafted polymers. In this case, we followed the consideration of Block et al. [62]  
285 and considered the PEO as only physisorbed on the surface of the silica particles. Hence,  
286  $L$  can be redefined as the thickness of the adsorbed PEO layer [62, 63]. In addition, the  
287 parameter  $s$  is originally defined as the average distance between two anchoring, grafted  
288 chains. Again, since the polymer was treated as physisorbed on the surface of the  
289 particles; hence, the steric force was considered to originate from the opposing loops  
290 and tails [62, 63]. Therefore, the parameter  $s$  may provide information on the average  
291 density of tails and loops of the adsorbed polymer [62, 63]. For the fitting, the  
292 parameters  $s$  and  $L$  were kept constant with a value of 75 nm and 198 nm, respectively.

293 As shown in Fig. 3, the AdG model showed good agreement with the measured force  
294 curve without adding the electrostatic forces, implying that the model is sufficient to  
295 describe the steric forces generated by the adsorbed polymer layer for both salt  
296 concentrations. These findings are fairly intuitive as the adsorbed polymer layers are  
297 thicker than the double-layer structure. Hence, the high molecular weight PEO provides  
298 a steric repulsion by the adsorbed polymer layer's opposing tails and/or loops.

299 Additionally, depletion was not observed in this study, as was previously observed [39],  
300 probably due to the concentration used in the present study. Depletion usually occurs at  
301 overdose polymer concentration, where the concentration of free polymers in the  
302 solution is relatively high, thereby increasing the osmotic pressure between the particles  
303 upon approach.

304 According to the AdG model, several pieces of information could be obtained.  
305 Firstly, the layer thickness of the adsorbed polymer layer was estimated to be around  
306  $2R_g - 3R_g$  for both salt concentrations. This observation was rather consistent and within  
307 the range of the previous studies, as the range of steric forces can be as several times as  
308  $R_g$  [42, 65–67]. Meanwhile, our previous study on the kinetics of PEO adsorption onto  
309 silica surfaces showed a hydrodynamic layer thickness of around  $1.3R_g$  at 50 ppm for  
310 the same molecular weight polymer [47]. Secondly, the parameter  $s$  was not affected  
311 much by the salt concentrations. However, the obtained parameter  $s$  was slightly higher  
312 than those for the grafted polymer case and in molecular dynamics simulations, with a  
313 value of around 3-18 nm [36, 68]. This is reasonable as the polymers in this study were  
314 only physisorbed onto the surface, and parameter  $s$  may be from the average density of  
315 tails and loops of the adsorbed polymer. On the other hand, Klein and Luckham  
316 obtained a value of  $s$  to be 11.0 nm for physisorbed PEO on mica surfaces[66]. In the  
317 case of physisorbed poly(styrene sulfonate), the value of  $s$  was within 50-60 nm [62,  
318 63], while Mohamad et al.[69] reported the value of  $s$  around 30-44 nm for the case of  
319 pseudo-brush poly(diallyl dimethylammonium chloride) (PDADMAC), which were  
320 comparable to our fitted value of  $s$ . Hence, we attribute the steric interactions were  
321 caused by the dangling loops and tails of the adsorbed PEO layer.

#### 322 **4. Conclusion**

323 The present study provides long-range force measurements between silica particles  
324 without and with nonionic PEO polymer layers at different molecular weights. In  
325 samples without PEO, the force profiles can be quantitatively interpreted in terms of  
326 DLVO theory, provided by the parameters describing the surface properties of the  
327 particles. This quantitative comparison between the experimental and theoretical  
328 features provides strong support for the applicability of the methodology for the force  
329 measurements in the presence of adsorbed PEO layer. In the presence of adsorbed PEO  
330 layer, the addition of low molecular weight PEO did not affect the double-layer  
331 structure. Based on this observation, we corroborate the notion that the reduction in the  
332 magnitude of the zeta potential in the presence of neutral polymer can be attributed to  
333 the shift of the shear plane from the hydrodynamic point of view.

#### 334 **Author Contributions**

335 **Lester C. Geonzon:** Conceptualization; Investigation; Methodology; Software; Data  
336 curation; Formal analysis; Validation; Visualization; Writing-original draft; Writing-  
337 review & editing. **Motoyoshi Kobayashi:** Supervision; Conceptualization;  
338 Methodology; Formal analysis; Visualization; Writing-original draft; Writing-review &  
339 editing; Resources; Funding acquisition; Project administration. **Takuya Sugimoto:**  
340 Formal analysis; Writing-review & editing; **Yasuhisa Adachi:** Supervision, Formal  
341 analysis; Writing-review & editing Resources; Funding acquisition; Project  
342 administration.



343 **Conflicts of interest**

344 There are no conflicts of interest to declare.

345 **Acknowledgment**

346 The authors are grateful for the financial support of JSPS KAKENHI Grant Number  
347 20F20388, 21K14939, 22H00387 and 19H03070.

348 **Reference**

- 349 1. Hiemenz PC, Rajagopalan R (1997) Principles of Colloid and Surface Chemistry,  
350 3rd ed. Marcel Dekker, Inc
- 351 2. Sone I, Hosoi M, Geonzon LC, et al (2022) Gelation and network structure of  
352 acidified milk gel investigated at different length scales with and without  
353 addition of iota-carrageenan. Food Hydrocoll 123:107170.  
354 <https://doi.org/10.1016/j.foodhyd.2021.107170>
- 355 3. Kim U, Carty WM (2016) Effect of polymer molecular weight on adsorption and  
356 suspension rheology. J Ceram Soc Japan 124:484–488.  
357 <https://doi.org/10.2109/jcersj2.15219>
- 358 4. Sis H, Birinci M (2009) Effect of nonionic and ionic surfactants on zeta potential  
359 and dispersion properties of carbon black powders. Colloids Surfaces A  
360 Physicochem Eng Asp 341:60–67.  
361 <https://doi.org/10.1016/j.colsurfa.2009.03.039>
- 362 5. Doan THY, Lim VH, Adachi Y, Pham TD (2021) Adsorption of Binary Mixture  
363 of Highly Positively Charged PTMA5M and Partially Negatively Charged PAA  
364 onto PSL Particles Studied by Means of Brownian Motion Particle Tracking and

- 365 Electrophoresis. Langmuir 37:12204–12212.  
366 <https://doi.org/10.1021/acs.langmuir.1c02160>
- 367 6. Szilagyı I, Trefalt G, Tiraferri A, et al (2014) Polyelectrolyte adsorption,  
368 interparticle forces, and colloidal aggregation. *Soft Matter* 10:2479–2502.  
369 <https://doi.org/10.1039/c3sm52132j>
- 370 7. Zaman AA (2000) Effect of polyethylene oxide on the viscosity of dispersions  
371 of charged silica particles: Interplay between rheology, adsorption, and surface  
372 charge. *Colloid Polym Sci* 278:1187–1197.  
373 <https://doi.org/10.1007/s003960000385>
- 374 8. Flerer GJ, Stuart MAC, Scheutjens JMHM, et al (1998) *Polymers at Interfaces*,  
375 1st ed. Springer, Dordrecht
- 376 9. Ruiz-Cabello FJM, Maroni P, Borkovec M (2013) Direct measurements of forces  
377 between different charged colloidal particles and their prediction by the theory  
378 of Derjaguin, Landau, Verwey, and Overbeek (DLVO). *J Chem Phys* 138:.  
379 <https://doi.org/10.1063/1.4810901>
- 380 10. Kobayashi M, Nitanaı M, Satta N, Adachi Y (2013) Coagulation and charging of  
381 latex particles in the presence of imogolite. *Colloids Surfaces A Physicochem*  
382 *Eng Asp* 435:139–146. <https://doi.org/10.1016/j.colsurfa.2012.12.057>
- 383 11. Kobayashi M, Yuki S, Adachi Y (2016) Effect of anionic surfactants on the  
384 stability ratio and electrophoretic mobility of colloidal hematite particles.  
385 *Colloids Surfaces A Physicochem Eng Asp* 510:190–197.  
386 <https://doi.org/10.1016/j.colsurfa.2016.07.063>
- 387 12. Lin W, Galletto P, Borkovec M (2004) Charging and aggregation of latex  
388 particles by oppositely charged dendrimers. *Langmuir* 20:7465–7473.  
389 <https://doi.org/10.1021/la049006i>

- 390 13. Valmacco V, Trefalt G, Maroni P, Borkovec M (2015) Direct force measurements  
391 between silica particles in aqueous solutions of ionic liquids containing 1-butyl-  
392 3-methylimidazolium (BMIM). *Phys Chem Chem Phys* 17:16553–16559.  
393 <https://doi.org/10.1039/c5cp02292d>
- 394 14. Popa I, Gillies G, Papastavrou G, Borkovec M (2010) Attractive and repulsive  
395 electrostatic forces between positively charged latex particles in the presence of  
396 anionic linear polyelectrolytes. *J Phys Chem B* 114:3170–3177.  
397 <https://doi.org/10.1021/jp911482a>
- 398 15. Adachi Y (1995) Dynamic aspects of coagulation and flocculation. *Adv Colloid*  
399 *Interface Sci* 56:1–31. [https://doi.org/10.1016/0001-8686\(94\)00229-6](https://doi.org/10.1016/0001-8686(94)00229-6)
- 400 16. Adachi Y, Kusaka Y, Kobayashi A (2011) Transient behavior of  
401 adsorbing/adsorbed polyelectrolytes on the surface of colloidal particles studied  
402 by means of trajectory analysis of Brownian motion. *Colloids Surfaces A*  
403 *Physicochem Eng Asp* 376:9–13. <https://doi.org/10.1016/j.colsurfa.2010.11.004>
- 404 17. Kawasaki S, Kobayashi M (2018) Affirmation of the effect of pH on shake-gel  
405 and shear thickening of a mixed suspension of polyethylene oxide and silica  
406 nanoparticles. *Colloids Surfaces A Physicochem Eng Asp* 537:236–242.  
407 <https://doi.org/10.1016/j.colsurfa.2017.10.033>
- 408 18. Kobayashi M (2020) An analysis on electrophoretic mobility of hydrophobic  
409 polystyrene particles with low surface charge density: effect of hydrodynamic  
410 slip. *Colloid Polym Sci* 298:1313–1318. [https://doi.org/10.1007/s00396-020-](https://doi.org/10.1007/s00396-020-04716-2)  
411 [04716-2](https://doi.org/10.1007/s00396-020-04716-2)
- 412 19. Sugimoto T, Cao T, Szilagyi I, et al (2018) Aggregation and charging of sulfate  
413 and amidine latex particles in the presence of oxyanions. *J Colloid Interface Sci*  
414 524:456–464. <https://doi.org/10.1016/j.jcis.2018.04.035>

- 415 20. Ohshima H, Sato H, Matsubara H, et al (2004) A theory of adsorption kinetics  
416 with time delay and its application to overshoot and oscillation in the surface  
417 tension of gelatin solution. *Colloid Polym Sci* 282:1174–1178.  
418 <https://doi.org/10.1007/s00396-004-1055-x>
- 419 21. Ohshima H (2006) *Theory of Colloid and Interfacial Electric Phenomena*, First  
420 Edit. Academic Press
- 421 22. Hill RJ, Saville DA (2005) “Exact” solutions of the full electrokinetic model for  
422 soft spherical colloids: Electrophoretic mobility. *Colloids Surfaces A*  
423 *Physicochem Eng Asp* 267:31–49.  
424 <https://doi.org/10.1016/j.colsurfa.2005.06.035>
- 425 23. Romero-Cano MS, Martín-Rodríguez A, de las Nieves FJ (2002) Electrokinetic  
426 behaviour of polymer colloids with adsorbed Triton X-100. *Colloid Polym Sci*  
427 280:526–532. <https://doi.org/10.1007/s00396-001-0643-2>
- 428 24. Zimmermann R, Romeis D, Bihannic I, et al (2014) Electrokinetics as an  
429 alternative to neutron reflectivity for evaluation of segment density distribution  
430 in PEO brushes. *Soft Matter* 10:7804–7809.  
431 <https://doi.org/10.1039/c4sm01315h>
- 432 25. Zimmermann R, Dukhin SS, Werner C, Duval JFL (2013) On the use of  
433 electrokinetics for unraveling charging and structure of soft planar polymer films.  
434 *Curr Opin Colloid Interface Sci* 18:83–92.  
435 <https://doi.org/10.1016/j.cocis.2013.02.001>
- 436 26. Langlet J, Gaboriaud F, Gantzer C, Duval JFL (2008) Impact of chemical and  
437 structural anisotropy on the electrophoretic mobility of spherical soft multilayer  
438 particles: The case of bacteriophage MS2. *Biophys J* 94:3293–3312.  
439 <https://doi.org/10.1529/biophysj.107.115477>

- 440 27. Trefalt G, Palberg T, Borkovec M (2017) Forces between colloidal particles in  
441 aqueous solutions containing monovalent and multivalent ions. *Curr Opin*  
442 *Colloid Interface Sci* 27:9–17. <https://doi.org/10.1016/j.cocis.2016.09.008>
- 443 28. Moazzami-Gudarzi M, Adam P, Smith AM, et al (2018) Interactions between  
444 similar and dissimilar charged interfaces in the presence of multivalent anions.  
445 *Phys Chem Chem Phys* 20:9436–9448. <https://doi.org/10.1039/c8cp00679b>
- 446 29. Kobayashi M, Juillerat F, Galletto P, et al (2005) Aggregation and charging of  
447 colloidal silica particles: Effect of particle size. *Langmuir* 21:5761–5769.  
448 <https://doi.org/10.1021/la046829z>
- 449 30. Furusawa K, Chen Q, Tabori N (1990) A new reference sample for  
450 microelectrophoresis. *J Colloid Interface Sci* 137:456–461.  
451 [https://doi.org/10.1016/0021-9797\(90\)90420-S](https://doi.org/10.1016/0021-9797(90)90420-S)
- 452 31. K. G. Mathai, Ottewill RH (1966) Stability of hydrophobic sols in the presence  
453 of non-ionic surface-active agents. Part 1.—Electrokinetic and adsorption  
454 measurements on silver iodide sols and suspensions. *Trans Faraday Soc* 62:750–  
455 758
- 456 32. Espasa-Valdepeñas A, Vega JF, Cruz V, et al (2021) Revisiting Polymer-Particle  
457 Interaction in PEO Solutions. *Langmuir* 37:3808–3816.  
458 <https://doi.org/10.1021/acs.langmuir.0c02715>
- 459 33. Garvey MJ, Tadros TF, Vincent B (1976) A comparison of the adsorbed layer  
460 thickness obtained by several techniques of various molecular weight fractions  
461 of poly(vinyl alcohol) on aqueous polystyrene latex particles. *J Colloid Interface*  
462 *Sci* 55:440–453. [https://doi.org/10.1016/0021-9797\(76\)90054-0](https://doi.org/10.1016/0021-9797(76)90054-0)
- 463 34. Van Heiningen JA, Hill RJ (2011) Poly(ethylene oxide) adsorption onto and  
464 desorption from silica microspheres: New insights from optical tweezers

- 465 electrophoresis. *Macromolecules* 44:8245–8260.  
466 <https://doi.org/10.1021/ma2003486>
- 467 35. Stuart MAC, Waajen FHWH, Dukhin SS (1984) Electrokinetic effects of  
468 adsorbed neutral polymers. *Colloid Polym Sci* 262:423–426.  
469 <https://doi.org/10.1007/BF01410263>
- 470 36. Tadros T (2011) Interaction forces between adsorbed polymer layers. *Adv*  
471 *Colloid Interface Sci* 165:102–107. <https://doi.org/10.1016/j.cis.2011.02.002>
- 472 37. van der Beek GP, Stuart MAC (1988) The hydrodynamic thickness of adsorbed  
473 polymer layers measured by dynamic light scattering: effects of polymer  
474 concentration and segmental binding strength. *J Phys Fr* 49:1449–1454.  
475 <https://doi.org/10.1051/jphys:019880049080144900>
- 476 38. Flood C, Cosgrove T, Howell I, Revell P (2006) Effects of electrolytes on  
477 adsorbed polymer layers: Poly(ethylene oxide)-silica system. *Langmuir*  
478 22:6923–6930. <https://doi.org/10.1021/la060724+>
- 479 39. Wei X, Gong X, Ngai T (2013) Interactions between solid surfaces mediated by  
480 polyethylene oxide polymers: Effect of polymer concentration. *Langmuir*  
481 29:11038–11045. <https://doi.org/10.1021/la401671m>
- 482 40. Al-Hashmi AR, Luckham PF (2012) Using atomic force microscopy to probe the  
483 adsorption kinetics of poly(ethylene oxide) on glass surfaces from aqueous  
484 solutions. *Colloids Surfaces A Physicochem Eng Asp* 393:66–72.  
485 <https://doi.org/10.1016/j.colsurfa.2011.10.025>
- 486 41. Giesbers M, Kleijn JM, Flerer GJ, Cohen Stuart MA (1998) Forces between  
487 polymer-covered surfaces: A colloidal probe study. *Colloids Surfaces A*  
488 *Physicochem Eng Asp* 142:343–353. [https://doi.org/10.1016/S0927-](https://doi.org/10.1016/S0927-7757(98)00366-5)  
489 [7757\(98\)00366-5](https://doi.org/10.1016/S0927-7757(98)00366-5)

- 490 42. Owen RJ, Crocker JC, Verma R, Yodh AG (2001) Measurement of long-range  
491 steric repulsions between microspheres due to an adsorbed polymer. *Phys Rev E*  
492 - *Stat Physics, Plasmas, Fluids, Relat Interdiscip Top* 64:6.  
493 <https://doi.org/10.1103/PhysRevE.64.011401>
- 494 43. Gong X, Wang Z, Ngai T (2014) Direct measurements of particle–surface  
495 interactions in aqueous solutions with total internal reflection microscopy. *Chem*  
496 *Commun* 50:6556–6570. <https://doi.org/10.1039/c4cc00624k>
- 497 44. Zębacz N, Wieczorek SA, Kalwarczyk T, et al (2011) Crossover regime for the  
498 diffusion of nanoparticles in polyethylene glycol solutions: Influence of the  
499 depletion layer. *Soft Matter* 7:7181–7186. <https://doi.org/10.1039/c0sm01357a>
- 500 45. Kalwarczyk T, Ziębacz N, Bielejewska A, et al (2011) Comparative analysis of  
501 viscosity of complex liquids and cytoplasm of mammalian cells at the nanoscale.  
502 *Nano Lett* 11:2157–2163. <https://doi.org/10.1021/nl2008218>
- 503 46. Geonzon LC, Kobayashi M, Adachi Y (2021) Effect of shear flow on the  
504 hydrodynamic drag force of a spherical particle near a wall evaluated using  
505 optical tweezers and microfluidics. *Soft Matter* 17:7914–7920.  
506 <https://doi.org/10.1039/d1sm00876e>
- 507 47. Geonzon LC, Kobayashi M, Sugimoto T, Adachi Y (2022) Study on the Kinetics  
508 of Adsorption of Poly(ethylene oxide) Onto A Silica Particle Using Optical  
509 Tweezers and Microfluidics. *Colloids Surfaces A Physicochem Eng Asp*  
510 642:128691. <https://doi.org/10.1016/j.colsurfa.2022.128691>
- 511 48. Pires LB, Ether DS, Spreng B, et al (2021) Probing the screening of the Casimir  
512 interaction with optical tweezers. *Phys Rev Res* 3:1–18.  
513 <https://doi.org/10.1103/PhysRevResearch.3.033037>
- 514 49. Ether DS, Pires LB, Umrath S, et al (2015) Probing the Casimir force with optical

- 515 tweezers. *Epl* 112:.. <https://doi.org/10.1209/0295-5075/112/44001>
- 516 50. Kawaguchi M, Mikura M, Takahashi A (1984) Hydrodynamic Studies on  
517 Adsorption of Polyethylene oxide) in Porous Media. 2.† Molecular Weight  
518 Dependence of Hydrodynamic Thickness. *Macromolecules* 17:2063–2065.  
519 <https://doi.org/10.1021/ma00140a032>
- 520 51. van der Beek GP, Cohen Stuart MA, Cosgrove T (1991) Polymer Adsorption and  
521 Desorption Studies via <sup>1</sup>H NMR Relaxation of the Solvent. *Langmuir* 7:327–  
522 334. <https://doi.org/10.1021/la00050a022>
- 523 52. Valmacco V, Elzbieciak-Wodka M, Besnard C, et al (2016) Dispersion forces  
524 acting between silica particles across water: Influence of nanoscale roughness.  
525 *Nanoscale Horizons* 1:325–330
- 526 53. Van Heiningen JA, Hill RJ (2011) Polymer adsorption onto a micro-sphere from  
527 optical tweezers electrophoresis. *Lab Chip* 11:152–162.  
528 <https://doi.org/10.1039/c005217p>
- 529 54. Wind B, Killmann E (1998) Adsorption of polyethylene oxide on surface  
530 modified silica - Stability of bare and covered particles in suspension. *Colloid*  
531 *Polym Sci* 276:903–912. <https://doi.org/10.1007/s003960050327>
- 532 55. Killmann E, Maier H, Baker JA (1988) Hydrodynamic layer thicknesses of  
533 various adsorbed polymers on precipitated silica and polystyrene latex. *Colloids*  
534 *and Surfaces* 31:51–71. [https://doi.org/10.1016/0166-6622\(88\)80182-3](https://doi.org/10.1016/0166-6622(88)80182-3)
- 535 56. Dijt JC, Stuart MAC, Fler GJ (1994) Kinetics of Adsorption and Desorption of  
536 Polystyrene on Silica from Decalin. *Macromolecules* 27:3207–3218.  
537 <https://doi.org/10.1021/ma00090a014>
- 538 57. Adachi Y, Wada T (2000) Initial stage dynamics of bridging flocculation of  
539 polystyrene latex spheres with polyethylene oxide. *J Colloid Interface Sci*



- 540 229:148–154. <https://doi.org/10.1006/jcis.2000.6964>
- 541 58. Adachi Y, Stuart MAC, Fokkink R (1994) Dynamic aspects of bridging  
542 flocculation studied using standardized mixing. *J Colloid Interface Sci* 167:346–  
543 351
- 544 59. G. J. Fleer, J. van Male and AJ (1999) Analytical Approximation to the  
545 Scheutjens–Fleer Theory for Polymer Adsorption from Dilute Solution. 2.  
546 Adsorbed Amounts and Structure of the Adsorbed Layer. *Macromolecules*  
547 32:845–862. <https://doi.org/https://doi.org/10.1021/ma980794q>
- 548 60. de Gennes PG (1987) Polymers at an interface; a simplified view. *Adv Colloid*  
549 *Interface Sci* 27:189–209. [https://doi.org/10.1016/0001-8686\(87\)85003-0](https://doi.org/10.1016/0001-8686(87)85003-0)
- 550 61. de Gennes PG (1980) Conformations of Polymers Attached to an Interface.  
551 *Macromolecules* 13:1069–1075. <https://doi.org/10.1021/ma60077a009>
- 552 62. Block S, Helm CA (2008) Conformation of poly(styrene sulfonate) layers  
553 physisorbed from high salt solution studied by force measurements on two  
554 different length scales. *J Phys Chem B* 112:9318–9327.  
555 <https://doi.org/10.1021/jp8020672>
- 556 63. Block S, Helm CA (2011) Equilibrium and nonequilibrium features in the  
557 morphology and structure of physisorbed polyelectrolyte layers. *J Phys Chem B*  
558 115:7301–7313. <https://doi.org/10.1021/jp112140t>
- 559 64. Braithwaite GJC, Luckham PF (1997) Effect of molecular weight on the  
560 interactions between poly(ethylene oxide) layers adsorbed to glass surfaces. *J*  
561 *Chem Soc - Faraday Trans* 93:1409–1415. <https://doi.org/10.1039/a606976b>
- 562 65. Klein J, Luckham PF (1984) Long-range attractive forces between two mica  
563 surfaces in an aqueous polymer solution. *Nature* 308:836–837.  
564 <https://doi.org/10.1038/308836a0>

- 565 66. Luckham PF, Klein J (1990) Forces between mica surfaces bearing adsorbed  
566 homopolymers in good solvents. The effect of bridging and dangling tails. J  
567 Chem Soc Faraday Trans 86:1363–1368. <https://doi.org/10.1039/FT9908601363>
- 568 67. Israelachvili JN (2011) Intermolecular and Surfaces Forces, Third Edit.  
569 Academic Press
- 570 68. Cordeiro RM, Zschunke F, Müller-Plathe F (2010) Mesoscale molecular  
571 dynamics simulations of the force between surfaces with grafted poly(ethylene  
572 oxide) chains derived from atomistic simulations. *Macromolecules* 43:1583–  
573 1591. <https://doi.org/10.1021/ma902060k>
- 574 69. Mohamad HS, Neuber S, Helm CA (2019) Surface Forces of Asymmetrically  
575 Grown Polyelectrolyte Multilayers: Searching for the Charges. *Langmuir*  
576 35:15491–15499. <https://doi.org/10.1021/acs.langmuir.9b01787>
- 577

Table 1. Estimated radius of gyration of PEO as a function of molecular weight

<b>Molecular weight (kg/mol)<sup>a</sup></b>	<b><i>R<sub>g</sub></i> (nm)</b>
20	7.6
100	17.1
1000	64.9

a Supplier Information

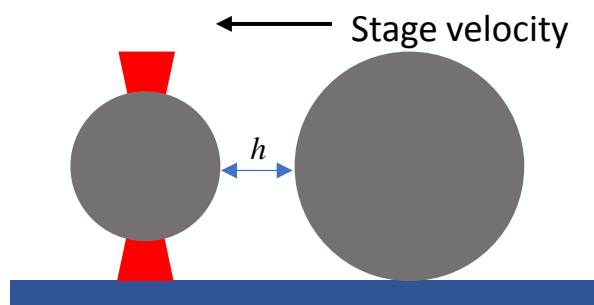


Figure 1. Schematic diagram of the silica-silica interaction. The large particle is adhered to the glass slide and displaced by moving the stage at a speed of  $0.02 \mu\text{m/s}$ .

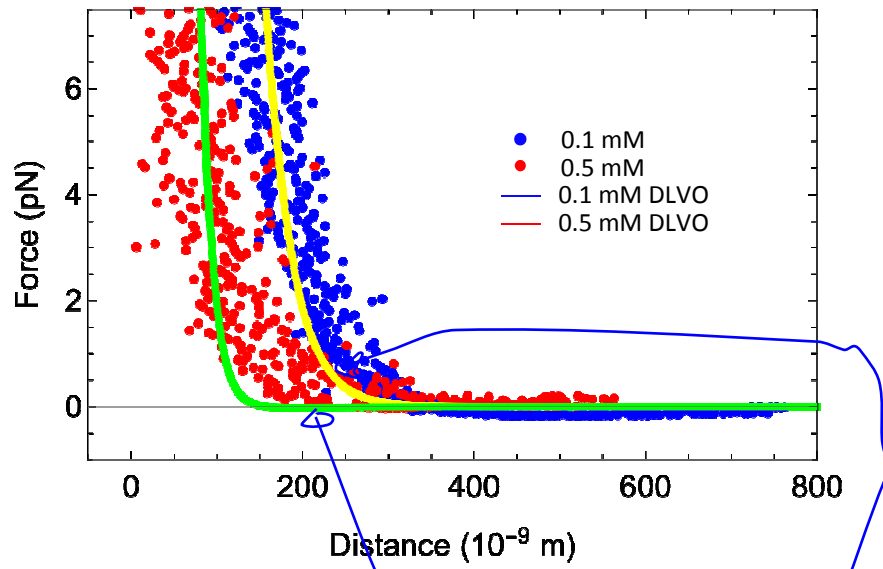


Figure 2. Effect of electrolyte concentration on the interaction between silica surfaces. Solid line: Theoretical curve using for 0.5 mM KCl (red), and for 0.1 mM KCl (blue).

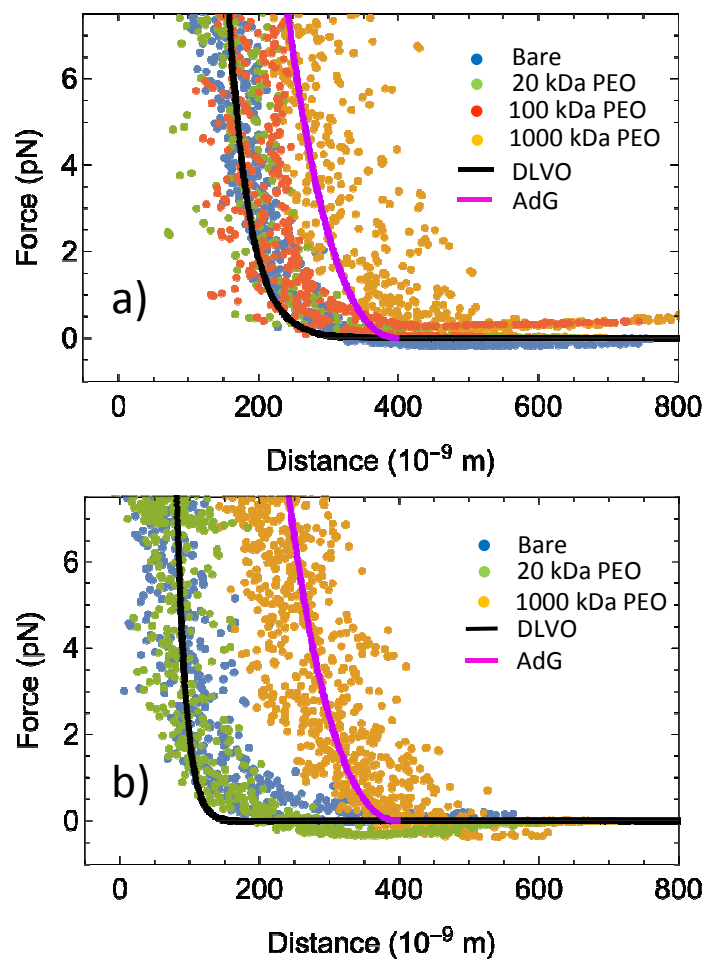


Figure 3. Effect of adsorbed PEO with different molecular weight on the interaction between silica surfaces: a) in 0.1 mM KCl, and b) in 0.5 mM KCl. Solid line: Theoretical curve using DLVO (Black) and AdG model (Orange).

Handwritten blue annotations: a bracket under the word "Orange" in the caption, and a question mark with a small 'P' below it.

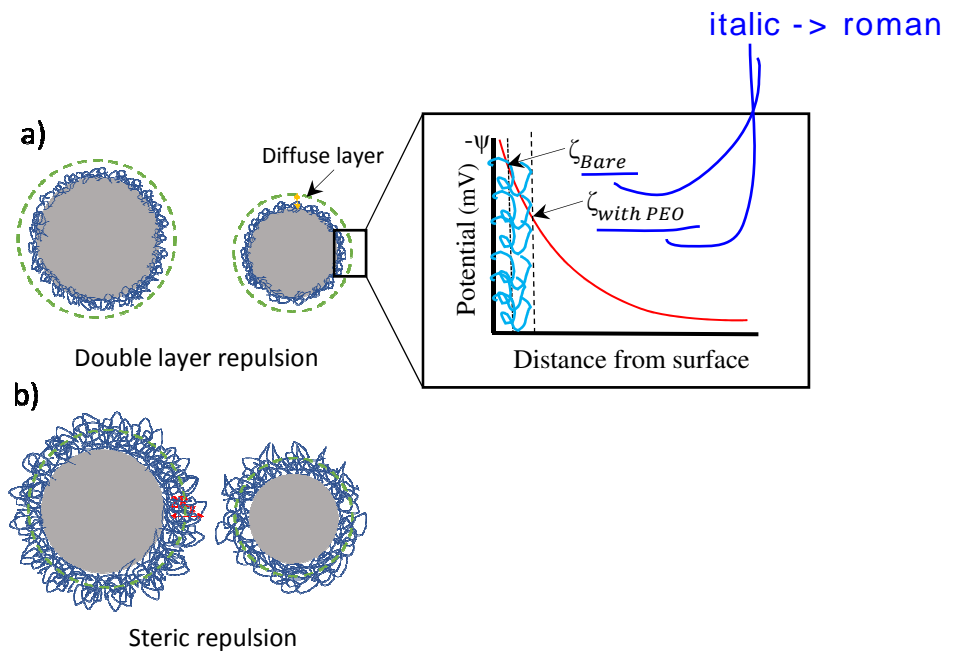


Figure 4. Schematic illustration of the interaction between particles with adsorbed neutral polymer. Inset of Figure 4a is the schematic potential distribution in the presence of PEO.